BBA - Molecular Basis of Disease 1870 (2024) 166915

Contents lists available at ScienceDirect

BBA - Molecular Basis of Disease

journal homepage: www.elsevier.com/locate/bbadis

Deciphering disease signatures and molecular targets in vascular Ehlers-Danlos syndrome through transcriptome and miRNome sequencing of dermal fibroblasts

Nicola Chiarelli [a,*], Valeria Cinquina [a], Paolo Martini [a], Valeria Bertini [a], Nicoletta Zoppi [a], Marina Venturini [b], Marco Ritelli [a], Marina Colombi [a]

[a] Division of Biology and Genetics, Department of Molecular and Translational Medicine, University of Brescia, 25121 Brescia, Italy
[b] Division of Dermatology, Department of Clinical and Experimental Sciences, Spedali Civili University Hospital Brescia, 25121 Brescia, Italy

ARTICLE INFO

Keywords:
Autophagy
Endoplasmic reticulum stress
Long non-coding RNAs
microRNAs
Transcriptome sequencing
Vascular Ehlers-Danlos syndrome

ABSTRACT

Vascular Ehlers-Danlos syndrome (vEDS) is a severe connective tissue disorder caused by dominant mutations in the *COL3A1* gene encoding type III collagen (COLLIII). COLLIII is primarily found in blood vessels and hollow organs, and its deficiency leads to soft connective tissues fragility, resulting in life-threatening arterial and organ ruptures. There are no current targeted therapies available. Although the disease usually results from COLLIII misfolding due to triple helix structure disruption, the underlying pathomechanisms are largely unknown. To address this knowledge gap, we performed a comprehensive transcriptome analysis using RNA- and miRNA-seq on a large cohort of dermal fibroblasts from vEDS patients and healthy donors. Our investigation revealed an intricate interplay between proteostasis abnormalities, inefficient endoplasmic reticulum stress response, and compromised autophagy, which may significantly impact the molecular pathology. We also present the first detailed miRNAs expression profile in patient cells, demonstrating that several aberrantly expressed miRNAs can disrupt critical cellular functions involved in vEDS pathophysiology, such as autophagy, proteostasis, and mTOR signaling. Target prediction and regulatory networks analyses suggested potential interactions among miRNAs, lncRNAs, and candidate target genes linked to extracellular matrix organization and autophagy-lysosome pathway. Our results highlight the importance of understanding the functional role of ncRNAs in vEDS pathogenesis, shedding light on possible miRNAs and lncRNAs signatures and their functional implications for dysregulated pathways related to disease. Deciphering this complex molecular network of RNA interactions may yield additional evidence for potential disease biomolecules and targets, assisting in the design of effective patient treatment strategies.

1. Introduction

Vascular Ehlers-Danlos syndrome (vEDS, OMIM #130050), a rare autosomal dominant connective tissue disorder with an estimated prevalence of 1/50.000–150.000, is the most severe form of EDS where affected individuals are at risk of life-threatening ruptures of medium- and large-sized arteries, the gastrointestinal tract, the gravid uterus, and other internal organs such as the liver or spleen [1–3]. vEDS is caused by mutations in the *COL3A1* gene encoding type III collagen (COLLIII), which provides strength and flexibility to blood vessels and membranes lining body cavities. COLLIII is primarily expressed in the walls of blood vessels and hollow organs, which explains why its deficiency can result in increased bruising, arterial and bowel rupture, and uterine, cervical, and vaginal fragility during pregnancy and delivery [1]. The diagnosis of

Abbreviations: COLLIII, type III collagen; DEGs, differentially expressed genes; DE-lncRNAs, differentially expressed lncRNAs; DE-miRNAs, differentially expressed miRNAs; ER, endoplasmic reticulum; ERAD, endoplasmic reticulum-associated degradation; ECM, extracellular matrix; FDR, false discovery rate; GO, Gene Ontology; HCA, hierarchical clustering analysis; lncRNAs, long non-coding RNAs; mTOR, mechanistic target of rapamycin; miRNAs, microRNAs; miRNA-seq, miRNA sequencing; ncRNAs, non-coding RNAs; PCA, principal component analysis; qPCR, quantitative polymerase chain reaction; RNA-seq, RNA sequencing; UPR, unfolded protein response; vEDS, vascular Ehlers-Danlos syndrome.

* Corresponding author at: Division of Biology and Genetics, Department of Molecular and Translational Medicine, University of Brescia, Viale Europa, 1125123 Brescia, Italy.
E-mail address: nicola.chiarelli@unibs.it (N. Chiarelli).

https://doi.org/10.1016/j.bbadis.2023.166915
Received 28 July 2023; Received in revised form 28 September 2023; Accepted 2 October 2023
Available online 10 October 2023

vEDS is based on the 2017 International Classification of EDS [4], which includes a family history with documented causative variant in *COL3A1*, a clinical history of arterial rupture, dissection or aneurysm, rupture of the large intestine, pregnancy complications at young ages, and carotid-cavernous fistula [1,3]. The biomechanical consequences of *COL3A1* mutations on tissue fragility extend beyond the vasculature. In fact, patients exhibit a range of clinical features including thin, translucent skin, spontaneous pneumothorax, acrogeria, hypermobile small joints, gingival recession due to fragile gingiva, early varicose veins, and a distinctive facial appearance [3]. The majority of disease-causing variants in vEDS are missense or splice site mutations that introduce a glycine substitution or result in an in-frame exon skip within the triple helical domain. These mutations cause misfolding of COLLIII in the endoplasmic reticulum (ER), leading to the retention of misfolded procollagen trimers in the cell and enlargement of ER vesicles [5]. Such mutations have a dominant negative effect on the protein by inhibiting extracellular accumulation of mature COLLIII [6]. A small proportion of affected individuals have null-mutations leading to *COL3A1* haploinsufficiency, which is associated with a delayed onset of complications by almost two decades and an overall milder phenotype [1,2].

Treatment for vEDS is currently limited to symptomatic measures, and surgical intervention is challenging due to the friable and fragile nature of tissues [7,8]. Preclinical research has been hindered by the lack of accurate animal models that can replicate disease mechanisms and vascular pathogenesis [8,9]. However, some progress has been made with the generation of knockin mouse models that mimic many of the vascular features of vEDS including arterial aneurysms and rupture [10,11]. From a biological perspective, the understanding of the specific functional implications of COLLIII deficiency in the extracellular matrix (ECM) and how alterations in the ECM affect underlying disease processes is limited. Our previous transcriptome analysis of dermal fibroblasts derived from a small group of patients revealed a dysregulated expression pattern of genes responsible for regulating collagen biosynthesis, ECM organization, and maintaining ER protein folding homeostasis. Protein studies showed that the altered distribution of the ER marker protein disulfide isomerase PDI, along with decreased levels of the COLLs-modifying enzyme FKBP22 [12,13], were consistent with disturbance in ER-related homeostasis and anomalies in collagen fiber structure and size [14].

In this study, we used comprehensive RNA sequencing to analyze transcriptome changes in a large cohort of dermal fibroblasts from vEDS patients and healthy donors. Our primary aim was to define a detailed molecular map that would reveal perturbed gene expression networks and cellular pathways contributing to the vEDS pathobiology. We also explored the potential involvement of non-coding RNAs (ncRNAs) such as microRNAs (miRNAs) and long non-coding RNAs (lncRNAs) as significant contributors to the underlying disease mechanisms. lncRNAs are a large group of non-protein coding transcripts exceeding 200 nucleotides in length that can modulate gene expression at various levels including epigenetic control, transcription, RNA processing, and translation [15]. miRNAs are small endogenous ncRNAs that are key regulators of gene expression, primarily influencing post-transcriptional processes by altering the translation and stability of target genes. They can precisely modulate various cellular processes related to disease onset and progression by targeting multiple components within a functional gene network [16].

Our transcriptome findings provide novel evidence of the impact of *COL3A1* defects on crucial cellular functions, which are associated with impaired adaptive cellular responses to counteracted ER stress and defective autophagy. Furthermore, we identified an abnormal expression profile of several miRNAs and lncRNAs that could potentially contribute to epigenetic mechanisms responsible for the multisystemic nature of vEDS. These novel insights improve the understanding of the disease pathogenesis, especially given the lack of prior molecular data on ncRNAs expression alterations. They also offer valuable clues that could facilitate translational and preclinical research efforts aimed at developing therapeutic options for patient management.

2. Patients, materials, and methods

2.1. Patients

This study was conducted in accordance with the Helsinki Declaration Principles and approved by the local Institutional Review Board (ASST degli Spedali Civili, Brescia, Italy, registration number NP5328). Eighteen adult vEDS patients (P1-P18, 10 females, 8 males) and 36 unrelated healthy donors (C1-C36, 30 females, 6 males) provided written informed consent for the study and skin biopsy in accordance with Italian bioethical standards. All patients were evaluated at the University Hospital Spedali Civili of Brescia's specialized outpatient clinic for Ehlers-Danlos syndromes and related connective tissue disorders. Patients were diagnosed according to the 2017 EDS nosology and molecularly characterized in our lab for a pathogenic dominant negative *COL3A1* variant [3]. Three patients (P1-P3) and all healthy individuals (C1-C36) were previously reported [13,17], whereas the other vEDS patients (P4-P18) were novel. Supplementary Table S1 lists the pathogenetic variants found in all enrolled patients along with an overview of their key clinical features.

2.2. Cell culture conditions

Fibroblast cultures were established in our lab according to standard protocols from skin biopsies obtained from the same site in the upper arms of vEDS patients and healthy donors. Fibroblasts were grown in vitro at 37 °C in a 5 % CO_2 atmosphere in Earle's Modified Eagle Medium supplemented with 2 mM L-glutamine, 10 % FBS, 100 μg/ml penicillin and streptomycin (Thermofisher Scientific, Rodano, Italy). Cells were expanded until full confluency and then harvested by 0.25 % trypsin/0.02 % EDTA treatment at the same passage number (from 3rd to 5th). Prior to transcriptome sequencing, we confirmed the typical ECM disorganization of type I, III, and V collagens, and fibronectin, along with the absence of α2β1 and α5β1 integrin expression, and the presence of organized αvβ3 integrin in all vEDS fibroblasts, through immunofluorescence analyses as previously reported [12,13].

2.3. RNA purification and transcriptome sequencing

Total RNA (comprising miRNAs) was purified from 18 vEDS patient and 36 control dermal fibroblasts grown for 72 h at 80 % of confluency using the miRNeasy kit (Qiagen, Milano, Italy). RNA quality and concentration were assessed with the Agilent 2100 Bioanalyzer (Agilent Technology, Cernusco sul Naviglio, Italy) and the Qubit fluorometer (Thermofisher Scientific, Rodano, Italy). To maximize statistical power, each transcriptome profile from both experimental groups included two biological replicates, for a total of 108 sequenced libraries. Transcriptome sequencing was carried out using the Thermofisher Scientific Ion Ampliseq Transcriptome Human Gene Expression kit (Thermofisher Scientific, Rodano, Italy), which targets by multiplexed PCR 18,574 protein-coding and 2228 ncRNAs (including lncRNAs), as previously reported [17]. Libraries were quantified using the Ion qPCR Library Quantification Kit, diluted to 100 pM and pooled at 8 samples per pool. Emulsion PCR and enrichment were performed using the Ion OneTouch2 system with ES. Libraries were loaded on an Ion 540 chip and sequenced with the Ion S5 instrument. Transcriptome Analysis Console 4.0 with the ampliSeqRNA plugin was used to identify differentially expressed genes (DEGs) through an ANOVA test with a fold-change threshold of 1.5 and an adjusted p-value ≤ 0.05 (p-value correction with Benjamini & Hochberg).

2.4. miRNome sequencing

miRNA libraries were prepared from 100 ng of total RNA purified

from 18 vEDS and 18 control cell strains using the QIAseq miRNA Library Kit (Qiagen, Milano, Italy). This library preparation kit incorporates unique molecular indexes during cDNA synthesis, which uniquely tag each strand before amplification, resulting in a more accurate reflection of endogenous miRNA levels by controlling for library amplification bias [18]. To ensure the accuracy and reproducibility of the data, a biological replicate was prepared for each patient and control sample, resulting in a total of 72 miRNA libraries. Libraries quality and concentration were assessed using the QIAxcel DNA high-sensitivity kit (Qiagen, Milano, Italy). Libraries were diluted to 4 nM and pooled at 6 samples per pool, followed by emulsion PCR and enrichment with the Ion OneTouch2 with ES system. Libraries were then loaded on an Ion 540 chip and sequenced with the Ion S5 instrument.

After read trimming using cutadapt v1.18 (adapter 3′ AACTGTAGGCACCATCAAT; adapter 5′ GTTCAGAGTTCTACAGTCCGACGATC), quantification was performed with the mirdeep2 pipeline [19] using as reference miRNAs and hairpins as defined in the miRBase 22.1. Reads shorter than 17 nucleotides were discarded. miRNAs with average expression below 20 counts across samples were excluded from further analysis. Differential expression analysis was performed with the DESeq2 R package v1.38.3 [20]. Differentially expressed miRNAs (DE-miRNAs) were identified by using an adjusted p-value ≤ 0.05 (p-value correction with Benjamini & Hochberg).

2.5. Biological classification of DEGs and miRNA targets prediction

DEGs were annotated based on the Gene Ontology (GO) and the Kyoto Encyclopedia of Genes and Genome (KEGG) terms using the DAVID database [21]. Functional enrichment analysis was performed with the ClueGO and CluePedia plugins of the Cytoscape platform to cluster dysregulated genes by their association with WikiPathways, KEGG, and REACTOME pathways annotation terms [22]. Being the number of input genes very high, network specificity was improved by setting strict parameters, as a GO level interval from 6 to 15 and a kappa-score (k) threshold of 0.7. A two-sided hypergeometric test was used considering only functional annotations with a step-down Bonferroni corrected p-value ≤ 0.01. MirWalk, TargetScan, microT-CDS, and miRTarBase databases were used to predict potential miRNAs-target genes. The Enrichr web tool was used to perform GO and pathway analyses to identify cellular pathways influenced by DE-miRNAs. Potential interactions among miRNAs, lncRNAs, and DEGs were obtained from miRNet 2.0 [23].

2.6. Quantitative PCR (qPCR)

Relative expression levels of a subset of DEGs were verified by qPCR using different RNA extractions obtained from patient and control fibroblasts. 3 μg of pooled vEDS (N. 18) and control (N. 36) RNA samples were reverse transcribed with random primers and qPCR was performed by SYBR Green dye and standard thermal cycling conditions using the QuantStudio 3 Real-Time PCR System (Thermofisher Scientific, Rodano, Italy). *ATP5B, CYC1, RPLP0,* and *YWHAZ* were used as housekeeping genes for mRNA normalization. Selected DE-miRNA relative expression levels were also verified using cDNA from reverse transcription of 20 ng of 18 pooled vEDS and 18 control RNA samples using the miRCURY LNA RT kit (Qiagen, Milano, Italy). qPCR was carried out with miRCURY LNA miRNA SYBR Green PCR kit (Qiagen, Milano, Italy), and miRCURY LNA miRNA PCR assay specific for each DE-miRNA (hsa-miR-15b-5p, ID: YP00204243; hsa-miR-16-5p, ID: YP00205702; hsa-miR-21-3p, ID: YP00204302; hsa-miR-24b-3p, ID: YP00204260; hsa-miR-29a-3p, ID: YP00204698; hsa-miR-29b-3p, ID: YP00204679; hsa-miR-138-5p, ID: YP00206078; hsa-miR-145-5p, ID: YP00204483; hsa-miR-195-5p, ID: YP00205869). *SNORD48* (ID: YP00203903), *U6 snRNA* (ID: YP00203907), *SNORA66* (ID: YP00203905), *SNORD44* (ID: YP00203902), and *SNORD38B* (ID: YP00203901) reference miRNAs were amplified for normalization of cDNA loading. Relative mRNA and miRNA expression levels were normalized to the geometric mean of references and analyzed using the $2^{-(\Delta\Delta Ct)}$ method. Statistical data were obtained with GraphPad Prism 8.0 by applying the unpaired Student's t-test.

3. Results

3.1. Exploring the transcriptomic landscape of vEDS dermal fibroblasts

To gain biological insights into dysregulated molecular mechanisms contributing to pathogenesis, we performed transcriptome sequencing on 18 dermal fibroblast strains from patients with vEDS and 36 cell strains from healthy donors. RNA samples from each group were sequenced twice as biological replicates to improve statistical power. We used ANOVA with a fold-change threshold of 1.5 and an FDR-adjusted p-value ≤ 0.05 to identify 3189 DEGs between vEDS and control fibroblasts: 3061 mRNAs and 128 ncRNAs. Out of the 128 identified ncRNAs, 64 were differentially expressed lncRNAs (DE-lncRNAs), comprising 13 upregulated and 51 downregulated transcripts, while 20 were small nucleolar RNAs with 17 upregulated and 3 downregulated transcripts. The remaining 44 were pseudogenes, of which 12 were upregulated and 32 downregulated (Supplementary Table S2).

Principal component analysis (PCA) and hierarchical clustering analysis (HCA) revealed the presence of two distinct clusters that efficiently separated vEDS patients from healthy individuals (Fig. 1A–B). The volcano plot indicated that 2618 DEGs (2532 mRNAs and 86 ncRNAs) were downregulated, while 571 showed increased expression (529 mRNAs and 42 ncRNAs) (Fig. 1C).

3.2. Transcriptome analysis revealed dysregulated biological functions potentially relevant for disease pathogenesis

To gain insight into the biological activities of the protein products of all DEGs, we performed GO enrichment analysis with DAVID. As shown in Fig. 2 and Supplementary Table S3, the most perturbed biological processes included mRNA splicing and processing, protein transport, translation, cell cycle regulation, autophagy, and chromatin remodeling. The most prevalent GO terms for molecular functions comprised protein binding, RNA binding, cadherin binding, structural constituent of ribosome, transcription corepressor activity, and ATP binding. Nucleoplasm, cytoplasm, mitochondrion, spliceosome, and endoplasmic reticulum were the most enriched cellular components GO terms. To further investigate the biological consequences of transcriptome alterations, we performed functional annotation clustering of all up- and downregulated DEGs (Table 1, Supplementary Table S4). Most of the functional clusters linked to downregulated DEGs were involved in mitochondrial processes, mRNA processing and translation, cell division, and DNA repair pathways. Patients' fibroblasts appear to have impaired ER homeostasis due to decreased expression of many protein-coding genes involved in ER protein folding quality control. These ER-associated genes encode molecular chaperones (*CANX*, *CCPG1*, *DNAJA2*, *DNAJA4*, *DNAJB5*, *DNAJC1*, *CCT3*, *CCT5*, *CCT8*), members of the protein disulfide isomerase family (*PDIA3*, *ERP29*, *P4HB*), as well as ER stress sensors (*ATF6*, *IRE1*, *XBP1*) that participate in the adaptive cellular ER stress responses, i.e., unfolded protein response (UPR) and ER-associated degradation (ERAD). Many genes (*ATP6V1A*, *ATP6AP2*, *ATP6V0A2*, *ATP6V1B2*, *ATP6V1H*, *ATP6V0C*, *ATP6V0A1*) related to the clathrin-coated vesicle membrane and components of the vacuolar ATPase (V-ATPase) made up another significantly enriched GO cluster. The decreased expression of *TFEB*, *ATG9A*, *ATG10*, *ATG12*, *VPS37A*, *VPS41*, *GABARAP*, *GABARAPL1*, *UVRAG*, *LAMP1*, and *CTSL* strongly suggests that the autophagy pathway may be compromised in vEDS cells.

According to the most enriched GO clusters (Table 1, Supplementary Table S4), the upregulated DEGs were primarily related to mitochondrial functions (e.g., *MRS2*, *MCUR1*, *COX4I1*, *ECI2*, *ETFA*, *GCSH*),

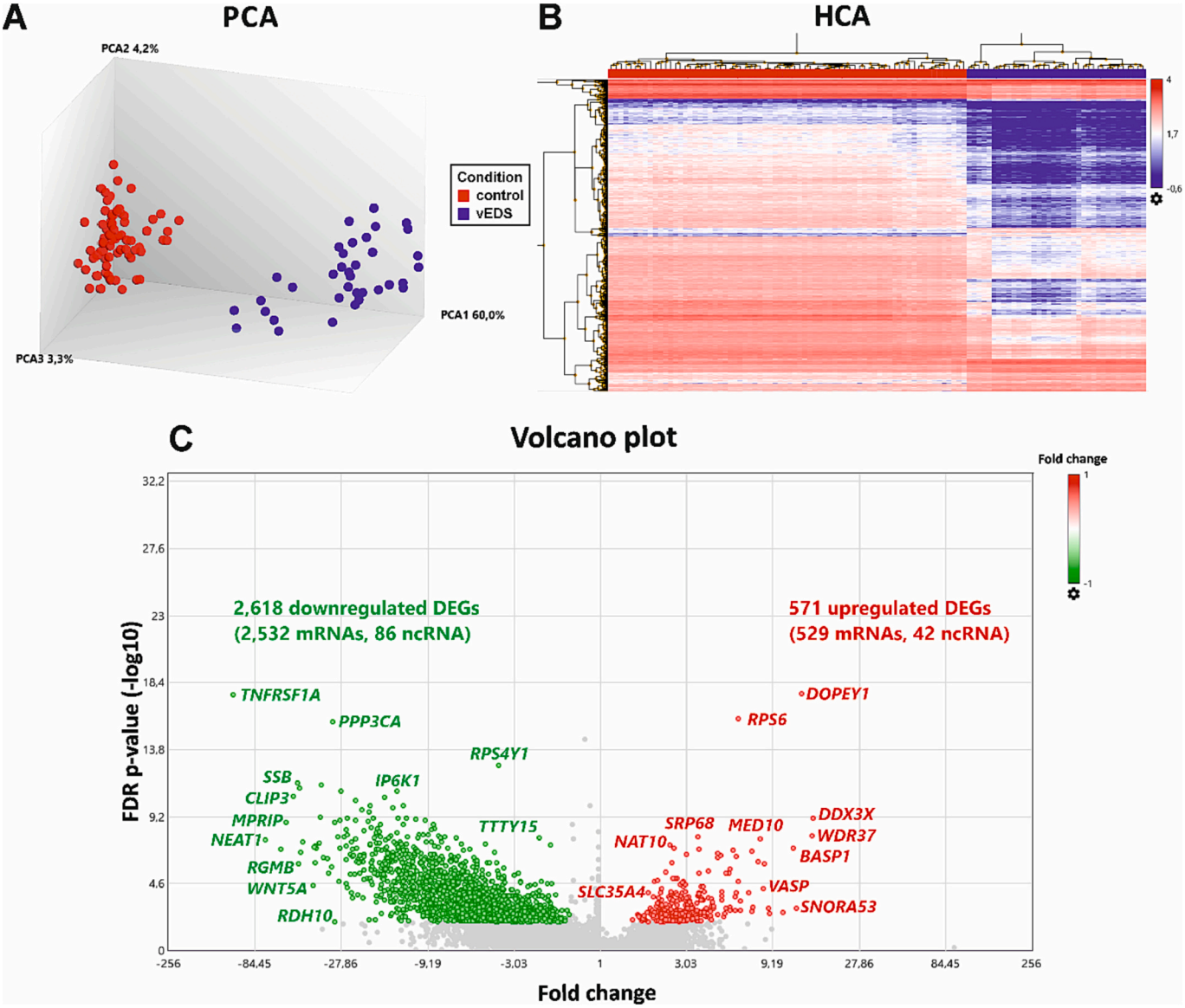

Fig. 1. Differential gene expression analysis. PCA plot of the 72 control (red dots) and 36 vEDS (blue dots) samples (**A**). Heatmap with downregulated genes in blue and upregulated genes in red for the 3189 DEGs found in vEDS vs. control showing two distinct transcript clusters that discriminate patient (blue bars) from control cells (red bars) (**B**). The Volcano plot illustrates the distribution of the 2618 downregulated (in green) and 571 upregulated (in red) DEGs (**C**). The plot represents expression values as fold change on the x-axis and -log10 FDR-adjusted *p*-value on the y-axis. A subset of DEGs is labeled with their gene symbols.

spliceosome and RNA processing (e.g., *SF3A1*, *RBM25*, *SNRPD2*, *LSM3*), and the mTOR signaling (e.g., *EIF2B5*, *EIF2S3*, *RPS6KB1*, *RPS6*, *AKT1*).

We also created functionally organized networks to gain a deeper understanding of the biological terms and functional pathways associated with gene expression changes (Fig. 3). Most of these biological networks were enriched by downregulated DEGs (Supplementary Table S5). Functional networks were primarily related to RNA metabolism and translation, mRNA splicing, ribosome, spliceosome, and mitochondrial ribosome. Additionally, cellular responses to stress and starvation, secretory and endocytic pathways, proteostasis, and catabolic processes like retrograde Golgi-to-ER traffic, membrane trafficking, endocytosis, ubiquitin-mediated proteolysis, proteasomal degradation, autophagy, and the mTOR signaling pathway, were all significantly enriched biological groups.

3.3. miRNome profiling revealed several differentially expressed miRNAs in pathways relevant to disease pathology

To investigate the potential role of miRNAs in disease mechanisms, we compared the entire miRNome of 18 vEDS dermal fibroblasts to 18 control cells. To improve statistical reliability, each sample from both groups was sequenced as biological replicates. By applying a $\log_2$ fold change threshold >1 or <-1, and an adjusted p-value ≤ 0.05, we identified 137 DE-miRNAs in patient vs. control fibroblasts. Of these, 71 miRNAs were downregulated, while 66 were upregulated (Supplementary Table S6).

To explore the functional relationship between DE-miRNAs and the altered gene expression profile of vEDS cells, we searched 4 miRNA-target prediction databases (microT-CDS, Targetscan, miRTarBase, and miRwalk) in addition to relevant literature sources providing information on the functional roles of these miRNAs. We then focused our research on a specific subset of DE-miRNAs, namely miR-15b-5p, miR-16-5p, miR-21-3p, miR-24-3p, miR-29a-3p, miR-29b-3p, miR-138-5p,

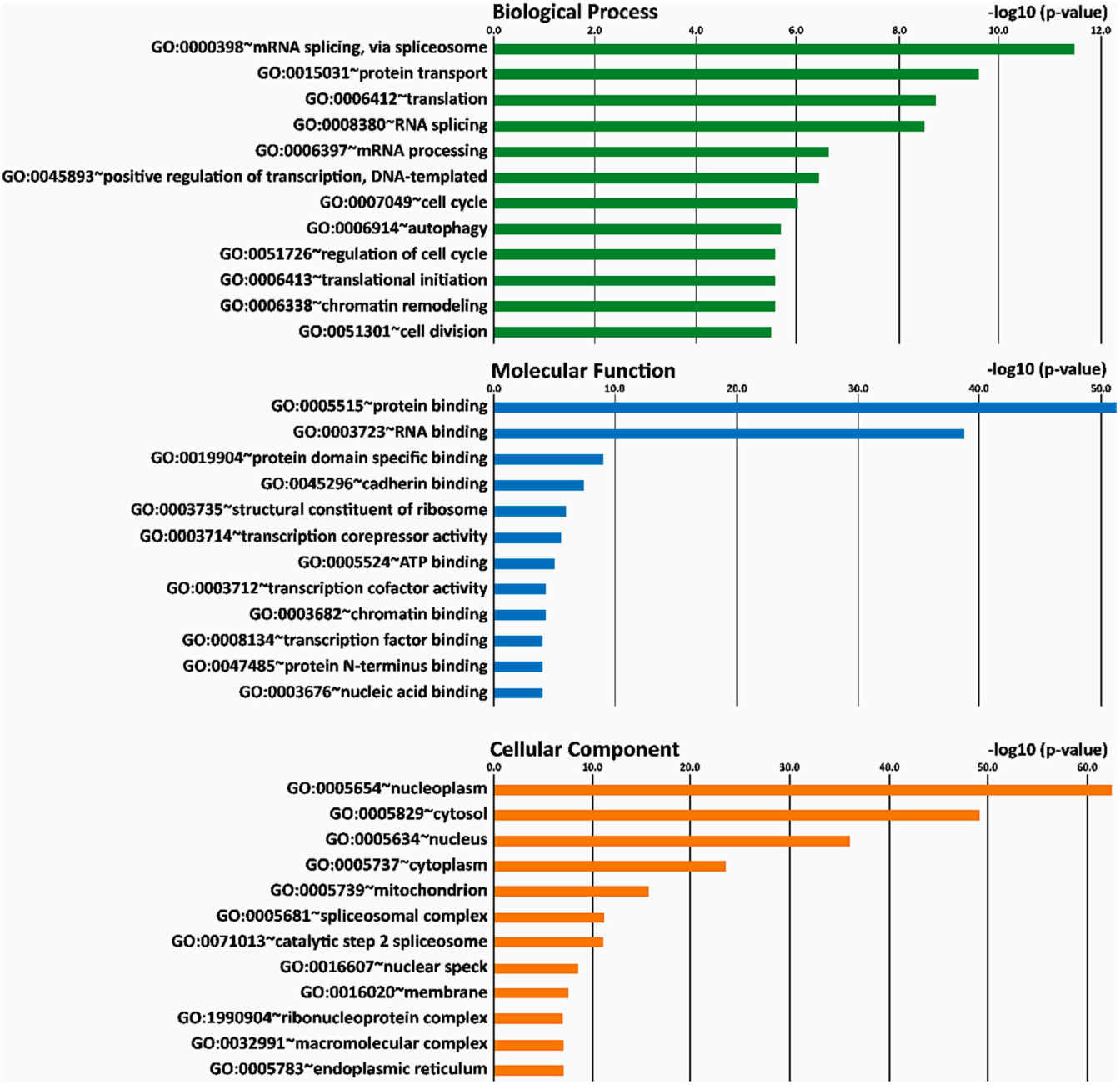

Fig. 2. DAVID functional gene enrichment analysis on DEGs (vEDS vs. control). Top 12 enriched GO terms for "Biological Process", "Molecular Function", and "Cellular Component" categories. GO terms for each category are plotted according to the -log10 *p*-value.

miR-145-5p, and miR-195-5p, which may play a biological role in dysregulated molecular mechanisms implicated in vEDS pathogenesis.

Our initial focus was on miR-29a-3p and miR-29b-3p due to their role in regulating critical cellular processes such as ECM remodeling into the vascular network, autophagy, cell proliferation, and apoptosis [24–26]. These biological processes are likely perturbed in vEDS cells and may contribute to the molecular pathogenesis of the disease.

To further investigate the role of these miRNAs, we searched for predicted miRNA targets among the 3189 DEGs. To reduce false positives, we only considered putative targets that were predicted by at least 2 of the 4 databases (Supplementary Table S7). We then merged the list of potential targets with the full list of DEGs to identify targets of miR-29a-3p and miR-29b-3p. For miR-29a-3p, this analysis revealed a total of 2586 potential target genes, distributed as follows: MicroT-CDS (984 targets), TargetScan (1260 targets), miRTarBase (242 targets), and miRwalk (1084 targets). Of these, 784 targets predicted by at least 2 of the 4 databases were merged with the DEGs, identifying 181 potential targets for miR-29a-3p (Fig. 4A). The analysis of miR-29b-3p identified 2996 potential target genes from MicroT-CDS (1002 targets), TargetScan (1264 targets), miRTarBase (240 targets), and miRwalk (487 targets), with 174 predicted targets obtained by intersecting the 749 targets predicted by at least 2 of the 4 databases with the DEGs (Fig. 4B).

To investigate how miR-29a-3p and miR-29b-3p contribute to the dysregulated cellular processes observed in patient cells, we performed GO and pathway enrichment analyses on their predicted target DEGs. GO analysis revealed that both miRNAs may alter fundamental biological functions like regulation of transcription by RNA polymerase II, negative gene expression regulation, miRNA-mediated gene silencing, translation regulation, heterochromatin organization, and ECM organization (Table 2, Supplementary Table S8). According to KEGG pathway

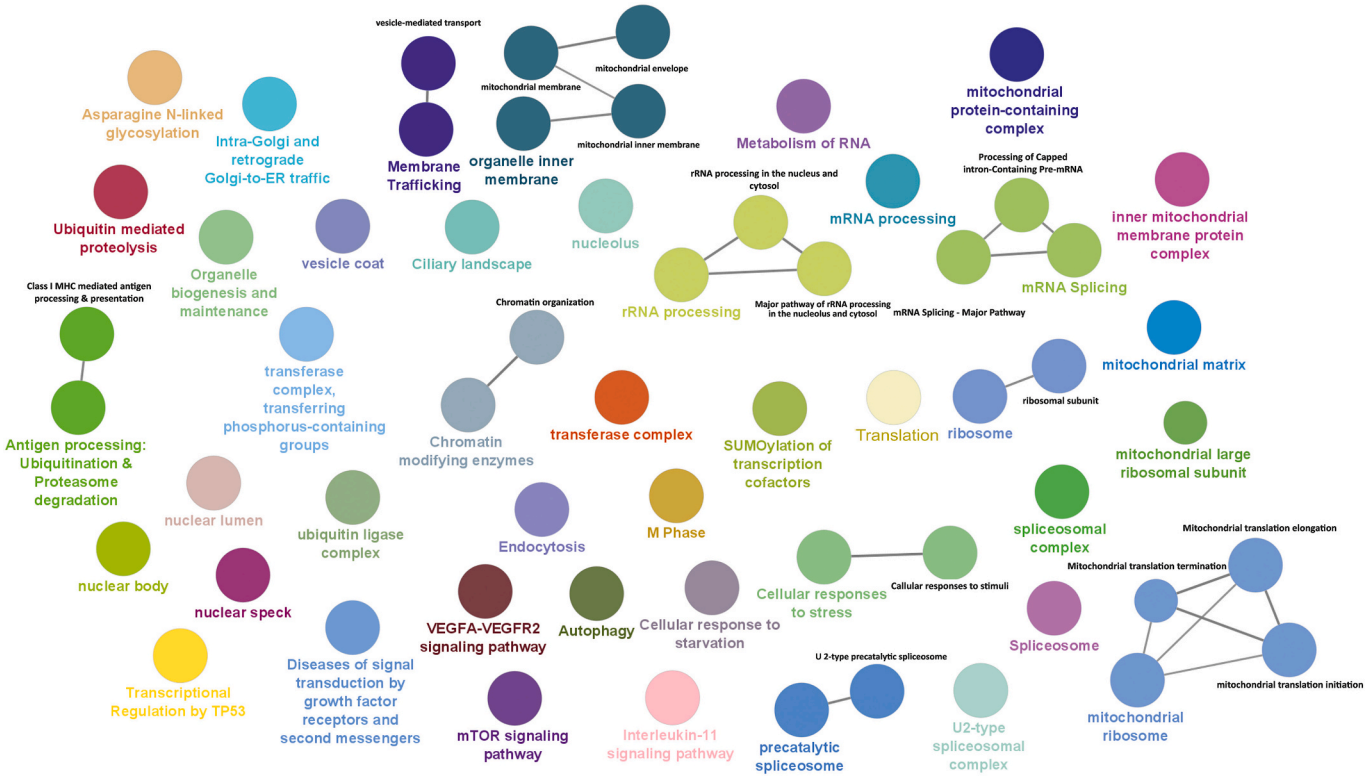

Fig. 3. Enriched biological networks based on the DEGs identified in vEDS fibroblasts, integrating GO-Biological Process with WikiPathways, KEGG, and Reactome databases. Terms (as nodes) are linked based on their κ score level (0.7), which defines term-term interactions (edges) and functional groups based on shared genes between the terms. Only enriched terms with Bonferroni step down-adjusted p-value ≤ 0.01 were considered.

analysis, miR-29a-3p and miR-29b-3p may impact several biological processes, such as autophagy, cellular senescence, RNA degradation, lipid and atherosclerosis, and lysine degradation. Moreover, both miRNAs may affect different signal transduction pathways including mTOR, FoxO, RIG-I-like receptor, and sphingolipid signaling pathways (Fig. 4A–B).

We also conducted functional enrichment analyses on the putative target DEGs of other relevant miRNAs, such as miR-15b-5p, miR-16-5p, miR-21-3p, miR-24-3p, miR-138-5p, miR-145-5p, and miR-195-5p (Supplementary Table 7). Consistent with the findings for miR-29a and miR-29b, also these miRNAs may be involved in pathways relevant to the disease pathophysiology (Supplementary Table S8). KEGG enrichment analysis indicated that some miRNAs may perturb significant cellular processes related to protein processing in ER, protein export, ubiquitin-mediated proteolysis, mitophagy, mTOR signaling (e.g., miR-15b, miR-16, miR-24, miR-145, miR-195), autophagy (e.g., miR-15b, miR-16, miR-21, miR-24, miR-195), cellular senescence (e.g., miR-21, miR-138), and p53 signaling pathway (e.g., miR-15b, miR-16, miR-24, miR-195) (Figs. S1 and S2). Together, the abnormal expression of several miRNAs in vEDS cells suggests epigenetic control over several DEGs and related biological processes, potentially impacting disease mechanisms.

3.4. Integrated analysis of potential miRNA-mRNA-lncRNA interactions

To identify lncRNAs that could act as competing endogenous RNAs, we searched the miRNet database [23] for co-regulatory expression networks involving lncRNAs, miR29a-3p, and miR-29b-3p. We identified 52 lncRNAs potentially acting as sponges for both miRNAs (Fig. 5A). RNA-seq analysis identified nuclear paraspeckle assembly transcript 1 (*NEAT1*) and HLA complex group 18 (*HCG18*) as downregulated transcripts, and MIRLET7B host gene (*MIRLET7BHG*) as upregulated in vEDS cells, with *NEAT1* being the most significantly downregulated ncRNA (Supplementary Table S2). Of note, *NEAT1* has been shown to act as molecular sponge for miR-29a-3p and miR-29b-3p to regulate their levels [27]. Therefore, we used the miRNet database to investigate the potential interactions between *NEAT1*, miR-29a, and miR-29b, and the 161 predicted target DEGs shared by both miRNAs (Supplementary Table S7). To improve the consistency of the results, we integrated experimentally validated miRNA target genes from the miRTarBase database [28], and focused on miRNA nodes that functioned as hubs. This analysis identified 213 predicted interactions between miR-29a and miR-29b and their potential targets. The targets of miR-29a or miR-29b included downregulated genes involved in collagen processing, protein degradation pathways, ECM remodeling, autophagy regulation and lysosomal acidification, as well as modulators of the Akt-mTOR signaling pathway (e.g., *P3H1*, *CAND1*, *COL5A1*, *COL7A1*, *COL15A1*, *LAMC1*, *ADAM12*, *ADAM19*, *TFEB*, *ATP6V1A, PTEN*) (Supplementary Table S9). A noteworthy observation is that *ATG9A* that is crucial for vesicle formation and elongation during autophagy was predicted to be a target of both miRNAs (Fig. 5B). Specifically, both miR-29a-3p and miR-29b-3p have been experimentally validated as targeting this gene in previous studies [27,29]. Additionally, also *NEAT1* has been reported to regulate the expression of *ATG9A* [27]. In addition to miR-29a and miR-29b, other dysregulated miRNAs in vEDS fibroblasts, such as miR-16-5p, miR-15a-5p and various members of the miR-let-7 family, were highly connected to several target DEGs (Fig. 5B, and Supplementary Table S9).

3.5. Validation of RNA-seq data by qPCR

We performed qPCR on a selection of dysregulated genes involved in significantly perturbed biological processes to validate transcriptome findings. We found that *COL3A1* structural mutations influence the expression of many transcripts involved in degradative endocytic trafficking and autophagy, including *TFEB*, *ATG9A*, *ATG10*, *ATG12*, *GABARAP*, *MAP1LC3A, STX17*, *UVRAG*, *LAMP1*, *STAT3*, *NLRX1*, and

Table 1
DAVID functional annotation clustering.

Cluster	Term description	Count	FDR	Selection of genes in the cluster
Selection of GO clusters enriched with downregulated DEGs				
1	GO:0005759 ~ mitochondrial matrix	58	1,13E-04	*ACADVL, ACAA2, FASTKD1, ECI1, FASTKD3, NDUFA10, ALKBH7, ALDH1L2, YARS2, MTG1, FPGS, NARS2, PMPCA, ACADM, NUDT13*
2	GO:0006397 ~ mRNA processing	39	0,00171	*SF3B2, RBM26, AKAP8L, SRA1, HNRPLL, YBX1, USP39, TSEN2, PRPF8, TSEN54, IWS1, ALKBH5, SNRPD1, PPP1R8, SAP18, RBM5*
3	GO:0051301 ~ cell division	58	0,00162	*RB1, DYRK3, CCNT1, HNRNPU, WASL, SMC3, USP39, TRIOBP, CDC73, SMC2, BABAM1, PPP1CC, CHMP1A, RCC1, PELO, NUDC*
4	GO:0006412 ~ translation	50	0,00117	*MRPS17, RPL5, MRPS15, MRPL36, RPL8, MRPL35, YARS2, RPL6, RPS15, MRPL3, RPL36AL, RPL35, RPL37, RPS11, RPL39, RPS9*
5	GO:0006457 ~ protein folding	32	0,01147	*TBCEL, WIPF1, GNAI1, DNAJB5, GRPEL2, CCT8, CCT5, TXNDC5, CCT3, PDIA3, HSPA9, PTGES3, TTC1, CLPX, PDCL3, DNAJC1, DNAJA4, CDC37, CANX, DNAJA2, ERP29, P4HB, ATF6, PPID*
6	GO:0030665 ~ clathrin-coated vesicle membrane	11	0,00493	*ATP6V1A, NECAP1, DENND1A, ATP6AP2, ATP6V1B2, ATP6V1H, AP3B1, ATP6V1E1, ATP6V0C, ATP6V1C1, ATP6V0A1*
7a	GO:0016236 ~ macroautophagy	18	0,006	*GABARAPL1, TSG101, SRC, EI24, MTMR14, VTA1, ATG10, VPS37A, STAM, GABARAP, ATG12, HGS, VPS41, CHMP2B, VTI1A, CHMP4B*
7b	GO:0000421 ~ autophagosome membrane	13	0,01043	*UVRAG, GABARAPL1, ATP6AP2, ATG9A, GABARAP, VMP1, LAMP1, JMY, CHMP2B, CHMP1A, CHMP4B, CHMP3, SNAP29*
Selection of GO clusters enriched with upregulated DEGs				
1	GO:0005739 ~ mitochondrion	68	0,03227	*MRS2, MCUR1, COX4I1, ECI2, ETFA, GCSH, METTL13, ANXA6, SLC25A40, TSPO, UQCRFS1, CAPN1, MRPL9, MTPAP, RMRP, USP48*
2	hsa03040:Spliceosome	16	0,01247	*TCERG1, PRPF38B, SF3A1, RBM25, PPIL1, HNRNPA3, ALYREF, LSM3, SNRPD2, DHX16, SNRPD3, SRSF7, BCAS2, HSPA1A, RBM22*
3	Skeletal muscle hypertrophy is regulated via AKT/mTOR pathway	6	0,00408	*EIF2B5, EIF2S3, RPS6KB1, RPS6, AKT1, EIF2S1*

TP53INP2 (Fig. 6A). We also confirmed expression changes of genes encoding subunits of V-ATPases and related to the mTOR signaling pathway, such as *AKT1*, *PTEN*, *NRAS*, *TSC1*, *TSC2*, *CASTOR1*, *CASTOR2*, *SLC38A9*, *MIOS*, *ATP6V1H*, *ATP6V0A1*, and *ATP6V0A2* (Fig. 6B). A considerable proportion of ER-associated genes, particularly those involved in protein folding, protein catabolism, COLLs processing, and ER homeostasis maintenance, including the UPR and ERAD pathways, showed significant expression changes (Fig. 6C). We also verified the differential expression of a specific group of upregulated (miR-29a-3p, miR-29b-3p, miR-15-5p, miR-16-5p, miR-21-3p, miR-138-5p) and downregulated (miR-24-3p, miR-145-5p, miR-195-5p) miRNAs (Fig. 6D). Likewise, we confirmed the decreased expression of the lncRNAs *NEAT1* and *HCG18*, which were chosen based on their predicted interactions with some of the DE-miRNAs (Fig. 5A). Overall, qPCR validation of all these transcripts supported the reliability of our RNA-seq results.

4. Discussion

The precise pathogenic mechanisms underlying vEDS remain poorly understood and there are currently no targeted therapies available for this condition. Our research study is the first attempt to reveal peculiar molecular signatures and disease mechanisms in a large cohort of dermal fibroblasts from vEDS patients and healthy individuals. By using an integrated transcriptomics approach, we have created a comprehensive map of complex gene expression networks in vEDS, which sheds light on intricate interactions within cellular signaling pathways. Our findings are particularly significant from a translational perspective, as there is currently no available molecular data describing alterations in the expression of miRNAs and lncRNAs in the context of disease mechanisms. Although we recognize that dermal fibroblasts may not perfectly replicate all vascular defects seen in vEDS, as other ECM-producing cells like vascular smooth muscle cells (VSMCs) and adventitial fibroblasts may exhibit different gene expression profiles, our cellular model can still provide valuable insights. Since vEDS patients exhibit significant cutaneous involvement and skin fragility similar to defects in vascular tissues, analyzing gene expression in dermal fibroblasts provides helpful clues regarding molecular pathways that could aid in explaining disease causes and guide future treatments.

The biological insights gleaned from our analyses are expected to provide valuable information for a considerable proportion of affected individuals. Indeed, all enrolled patients harbored *COL3A1* glycine substitutions and in-frame exon skipping, which are the most common types of mutations that cause the disease and are associated with a more severe clinical presentation [3,6,8]. In addition to their dominant negative effect on the ECM, such structural mutations in collagen molecules can cause ER stress by disrupting the proper protein turnover and ER homeostasis [30]. This disturbance triggers adaptive cellular responses, such as UPR, in the attempt to restore ER homeostasis by upregulating the expression of ER-resident chaperones to increase protein folding capacity, activating protein degradation pathways, while simultaneously reducing global protein synthesis [30,31]. Our previous protein and gene expression studies have indicated that abnormal COLLIII expression and its intracellular retention are associated with pathological ECM remodeling, insufficient proteostasis, and perturbed ER homeostasis [13,32]. In line with our previous works, the current RNA-seq data confirm and provide additional convincing evidence that

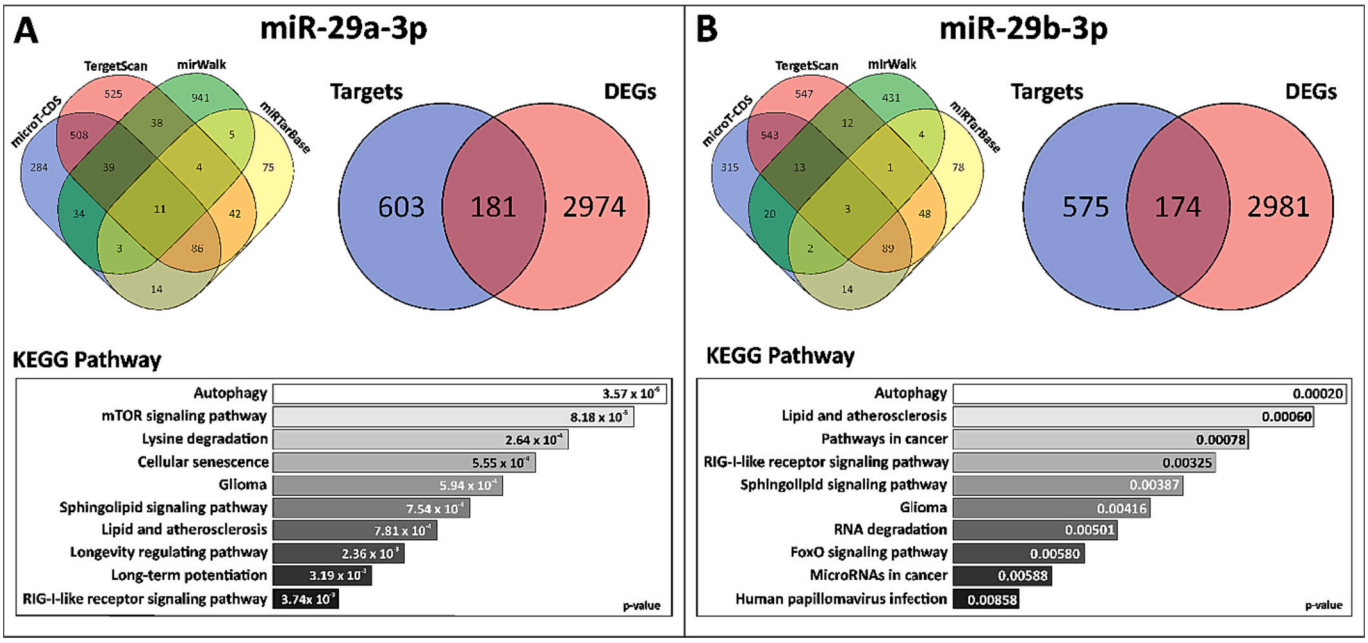

Fig. 4. Target prediction analysis for miR-29a-3p (**A**) and miR-29b-3p (**B**) by querying the microT-CDS, TargetScan, miRwalk, and miRTarBase databases. The predicted targets for both miRNAs were compared with the 3189 DEGs, identifying 181 and 174 targets for miR-29a-3p and miR-29b-3p, respectively. Functional enrichment analysis of target DEGs was performed by querying the EnrichR web tool. The KEGG pathway analysis results are shown in the bottom panel.

Table 2
The most representative GO terms for target DEGs of miR-29a and miR-29b.

Biological processes related to the aberrant expression of miR-29a-3p		
GO terms	p-Value	181 target DEGs
Regulation of transcription by RNA polymerase II (GO:0006357)	0.0001	***NFAT5***, *DDX3X*, ***KMT2A***, ***DOT1L***, ***EHMT1***, *GABPB1*, *ZBTB5*, *PPM1D*, ***GLIS2***, ***LRP6***
Negative regulation of gene expression (GO:0010629)	0.00162	***DNMT1***, ***BTG2***, *DDX3X*, ***SETDB2***, ***DICER1***, *PPM1D*, ***SIRT1***, ***REST***, ***SERBP1***, ***REL***, ***EPC1***, ***CPEB3***, ***PAIP2***, ***DCP2***
Heterochromatin organization (GO:0070828)	0,00432	***KDM5B***, ***KDM4B***, ***REST***, ***CBX5***, ***POLE3***, ***EHMT1***, ***HDGF***, ***SPTY2D1***, *SMARCA2*, ***SIRT1***
Negative regulation of signal transduction by p53 class mediator (GO:1901797)	0,04218	***MAPKBP1***, ***NLRX1***, ***RIOK3***, ***SIRT1***
Regulation of translation (GO:0006417)	0,04218	*RPS6KA3*, ***BTG2***, *DDX3X*, ***SERBP1***, ***LARP4***, ***CPEB3***, ***PAIP2***, *EIF2S1*

Biological processes related to the aberrant expression of miR-29b-3p		
GO terms	p-Value	174 target DEGs
Negative regulation of gene expression (GO:0010629)	0.00017	***BTG2***, *DDX3X*, ***SETDB2***, ***DNMT3A***, ***DICER1***, *PPM1D*, ***SIRT1***, ***CNOT1***, ***AGO1***, ***REL***, ***EPC1***, ***CPEB3***, ***DCP2***
Gene silencing by miRNA (GO:0035195)	0,00216	***CNOT6***, ***CNOT1***, ***AGO1***, *SNIP1*, ***DICER1***
Heterochromatin organization (GO:0070828)	0,00414	***SETDB2***, ***POLE3***, ***SIRT1***
Proteasomal Protein Catabolic Process (GO:0010498)	0,04346	*KLHDC3*, ***WDR26***, ***RMND5A***, ***FEM1B***, *DDI2*, ***MDM2***, *UBE2K*, ***SIRT1***
Extracellular matrix organization (GO:0030198)	0,04416	***ADAM19***, ***COL15A1***, ***COL5A1***, ***SH3PXD2A***, ***COL7A1***, ***ADAM12***, ***P3H1***, ***LAMC1***, ***NID2***

Downregulated DEGs are shown in bold.

ineffective proteostasis, unbalanced ER homeostasis, and compromised autophagy could substantially impact the molecular pathology driving the disease. Disruption of these key biological pathways necessary for maintaining cellular health supports our belief that an inadequate cellular response to ER stress likely plays an important role in vEDS pathomechanisms, as demonstrated in other collagen-related disorders [30,33–37]. The significant changes in the expression of numerous genes required for maintaining autophagy and normal protein folding observed in vEDS fibroblasts strongly corroborate this view. Indeed, many DEGs play pivotal roles at distinct stages of the autophagy-lysosome system, including vesicle formation and elongation (*TFEB*, *WIPI*, *MAP1LC3A*, *ATG9A*), autophagosome-lysosome fusion (*GABARAP*, *UVRAG*, *LAMP1*), and substrate degradation (*CTSL* and numerous V-ATPase subunit genes). V-ATPases are ATP-dependent proton pumps that create an acidic lysosomal environment required for proper degradation and turnover of cellular components and prevention of cytotoxic products accumulation within cells [38]. Among the above-mentioned autophagy-related genes, the transcription factor EB (*TFEB*) is recognized as a central regulator of lysosomal biogenesis and homeostasis [39]. By controlling the expression of numerous transcripts involved in autophagy and lysosome function, TFEB orchestrates a transcriptional program that controls key phases of the autophagic flux and lysosomal proteolysis [40,41]. Our transcriptome analysis revealed decreased expression not only of *TFEB*, but also many of its known downstream targets, including *ATG9A*, *UVRAG*, *LAMP1*, *CTSL*, and various V-ATPase subunit genes. All these genes have been well-characterized as being involved in these processes [40,42,43]. Therefore, our RNA-seq results strongly indicate a significant impairment of the entire autophagy-lysosome pathway in vEDS cells, which involves TFEB and several of its downstream target genes. Autophagy also serves as a cytoprotective mechanism during ECM detachment-induced apoptosis [44,45] and as an ER-phagy pathway for collagen quality control in collagen-producing cells [46,47]. Impaired autophagy can disrupt the normal ECM turnover, resulting in defective collagen proteostasis and perturbed ER homeostasis, leading to unresolved ER stress and activation of pro-apoptotic programs [48]. Our previous protein analyses of patients' fibroblasts support this finding, showing increased pro-apoptotic caspase enzymes and decreased anti-apoptotic Bcl-2

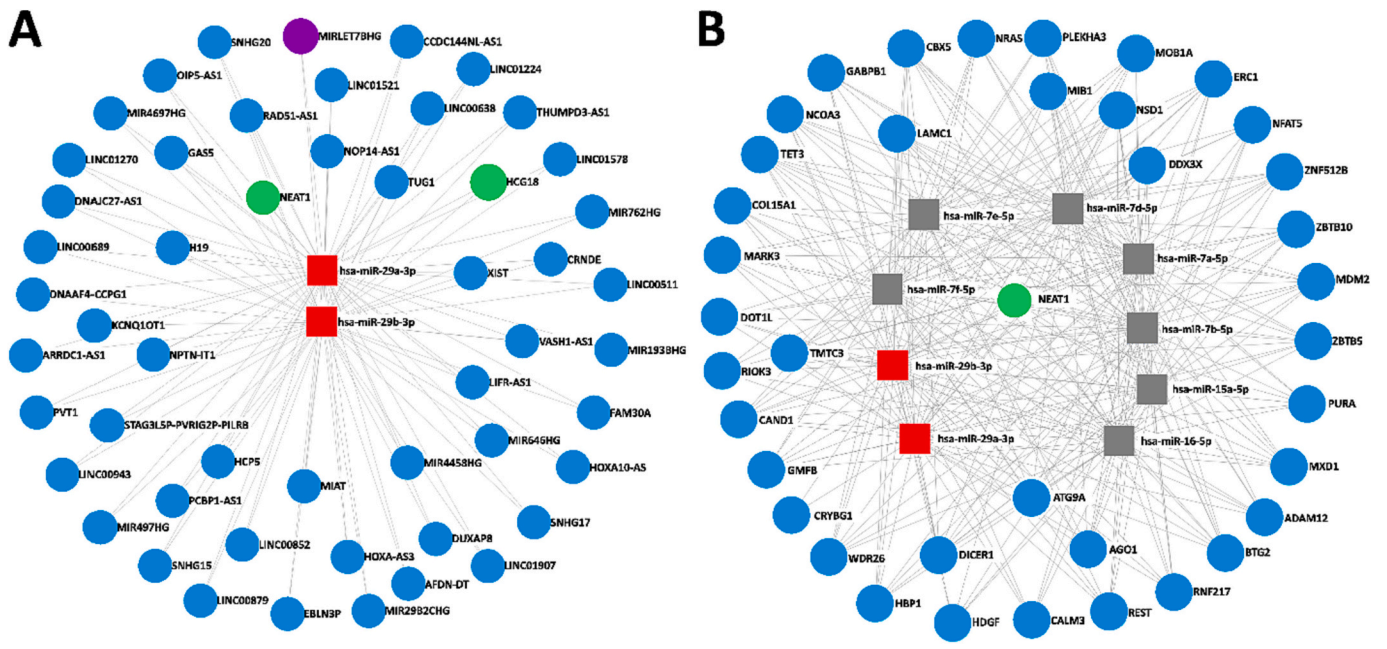

Fig. 5. Construction of a miRNA-mRNA-lncRNA interaction network. In silico prediction of co-regulatory lncRNA-miRNA networks involving miR-29a-3p and miR-29b-3p (**A**). Potential regulatory network involving DE-miRNAs-DEGs-DE-lncRNAs (**B**). Red squares indicate upregulation of miR-29a-3p and miR-29b-3p, green circles represent downregulation of lncRNAs *NEAT1* and *HCG18*, purple circle indicates upregulation of lncRNA *MIRLET7BHG*, and grey squares represent other DE-miRNAs. The miRNet 2.0 database was queried for the prediction analysis of ncRNA-mRNA interactions.

protein [49]. These data suggest that vEDS cells are more susceptible to apoptosis due to excessive ECM disorganization and defective ER homeostasis, which is most likely caused by reduced secretion and intracellular accumulation of abnormally folded COLLIII protein, leading to subsequent ER stress [12,13,32,49,50]. Despite previous findings showing enlarged ER in patients' skin biopsies [5,14], the nature of the altered proteostasis within the ER and its downstream molecular consequences remain poorly defined. The present findings could provide noteworthy evidence to address this gap in molecular understanding. Indeed, the discovery that a large portion of downregulated genes encode proteins essential for maintaining ER protein folding, such as molecular chaperones, protein folding enzymes, proteasome complex subunits, key ER stress sensors, and components of the UPR and ERAD pathways, provides additional evidence that patients' fibroblasts may fail to activate efficient defenses against defective ER homeostasis. Taken together, our current and previous research provides further support for the widely accepted view that *COL3A1* misfolding mutations disrupt the ECM network and reduce the bioavailability of several structural constituents, including other fibrillar collagens, fibronectin, and elastin, all of which are essential for the integrity of soft connective tissues, including vascular tissue [13,32]. As a result, misfolded COLLIII aggregates, along with intracellular accumulation of other misfolded ECM proteins, may hamper protein folding machinery, disrupting ER proteostasis, adaptive cellular stress responses, and autophagy (Fig. 7).

Additional hints from RNA-seq data point to a potential connection between the mammalian target of rapamycin (mTOR) pathway, impaired autophagic response, and insufficient lysosome clearance in vEDS cells. Various genes involved in the mTOR signaling, including *AKT1*, *PTEN*, *NRAS*, *TSC1*, *TSC2*, *CASTOR1*, *CASTOR2*, *SLC38A9*, and *MIOS*, showed significantly altered expression in patients' cells. These gene expression abnormalities may result in mTOR signaling dysregulation, which could then impact crucial cellular processes like protein quality control, autophagy, and lysosome function, all of which appear impaired in vEDS.

mTOR signaling controls different anabolic biological activities, including protein synthesis, lipid metabolism, and cell growth by interacting with particular adaptor proteins and forming multiprotein complexes called mTORC1 and mTORC2 [51]. mTOR also senses and responds to upstream signals like growth factors, nutrients, amino acids, and starvation [52], and acts as a transcriptional regulator controlling autophagy and lysosome degradation [42]. Moreover, it is crucial in coordinating TFEB phosphorylation, its subcellular localization and the expression of a specific set of TFEB-responsive genes involved in autolysosome formation and lysosomal acidification [38,53], including the downregulated DEGs *UVRAG*, *LAMP1*, and several V-ATPase subunit genes. A deeper understanding of the mTOR-mediated mechanisms governing autophagic and lysosomal events (e.g., by inhibiting TFEB nuclear translocation) could provide new insights into the precise role of this signaling network in disease pathways. Furthermore, epigenetic changes that result in altered expression of specific miRNAs identified in patients' fibroblasts could impact this potential molecular regulatory network linking mTOR signaling and autophagy-lysosomal pathway. Upregulated miR-15b-5p, miR-16-5p, miR-21-3p, miR-29a, and miR-29b may influence the intricate interaction between these two crucial biological processes by inhibiting the transcription of several associated genes [54,55]. By analyzing miRNA-target interactions, we discovered several interesting target genes of miR-29a-3p and miR-29b-3p. As previously demonstrated [27,29,56–59], both miR-29a and miR-29b may negatively regulate the expression of mTOR and autophagy-related genes like *TFEB*, *ATG9A*, *GABARAP*, *PTEN*, and *STAT3*, which are all downregulated in patients' cells. To further assess potential connections between DE-miRNAs, DE-lncRNAs, and DEGs, we built a regulatory interaction network. This analysis revealed that various miRNAs, including miR-29a and miR-29b, as well as lncRNAs like *NEAT1*, may compete to control the expression of different genes. Among the predicted targets, *ATG9A* was recognized as a potential co-regulated target of both miRNAs [27,29]. This gene encodes an integral membrane protein essential for the early stages of autophagosome formation [60]. Our observations are consistent with earlier experimental findings that demonstrated a close relationship between miR-29b-3p, *ATG9A*, and *NEAT1*, as well as their crucial role in controlling autophagy activation [27]. *NEAT1* acts as a competing endogenous RNA by sequestering miR-29b, leading to lower levels and reduced activity [27,61]. *NEAT1* contributes significantly to the autophagic flux

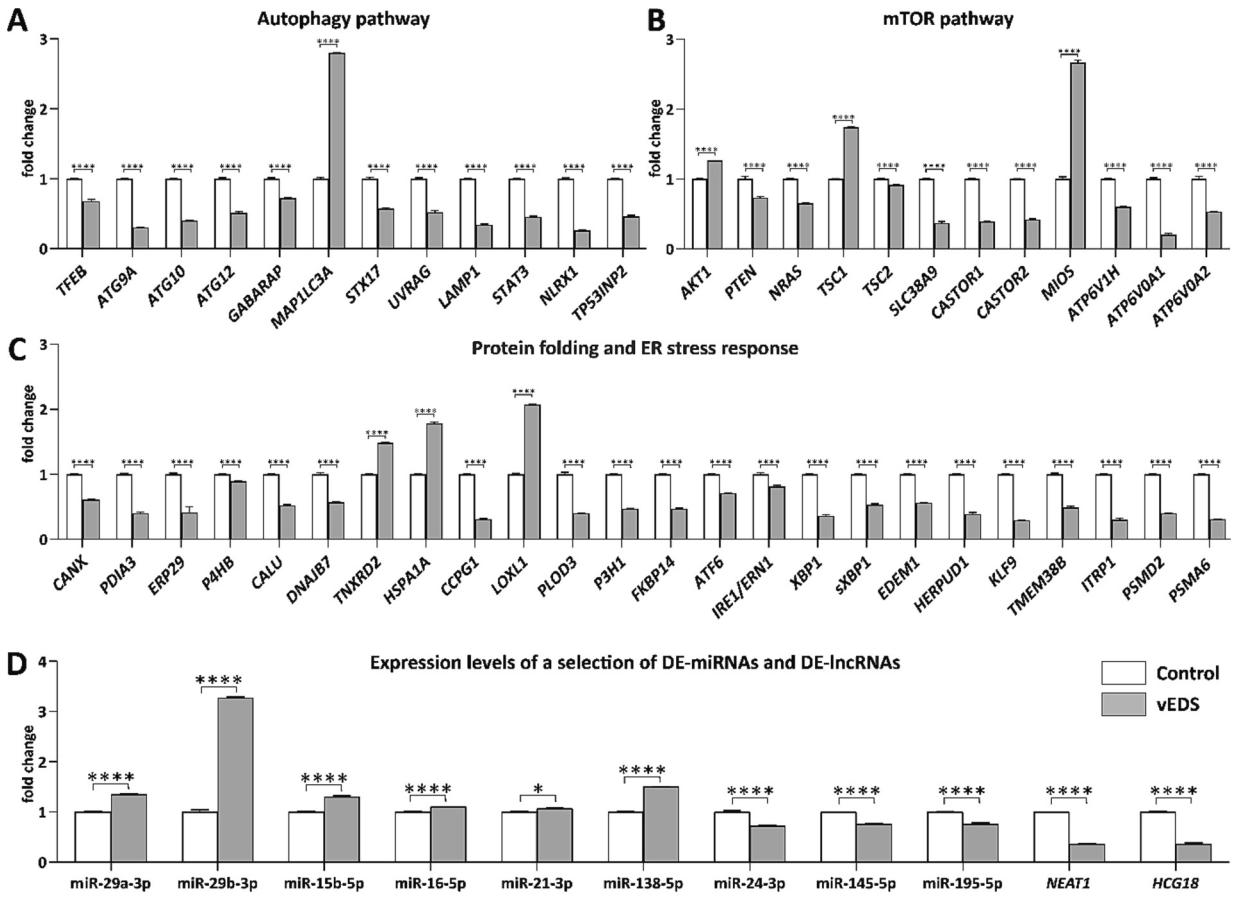

Fig. 6. qPCR validation of transcriptome findings. The relative mRNA expression levels of selected genes related to autophagy and lysosomal biogenesis (**A**), mTOR signaling pathway (**B**) and involved in protein folding, COLLs processing, ER homeostasis, ER stress response (UPR and ERAD pathways), and proteasome-mediated protein degradation (**C**) were determined using the $2^{-(\Delta\Delta Ct)}$ method normalized with the geometric mean of *ATP5B*, *CYC1, RPLP0*, and *YWHAZ* reference genes. Bars represent the mean ratio of target gene expression from pooled RNA samples of 18 vEDS and 36 control fibroblasts. Relative expression levels of a subset of DE-miRNAs and DE-lncRNAs identified in patients' cells (**D**). *SNORD48*, *U6 snRNA*, *SNORA66*, *SNORD44*, and *SNORD38B* reference miRNAs were used as endogenous controls for template normalization. Bars represent the mean ratio of expression levels from pooled RNA samples of 18 vEDS and 18 control cells. All qPCR analyses were carried out in quadruplicate in two independent experiments. Statistical significance between groups were determined using an unpaired Student's *t*-test and data are expressed as mean ± SEM (*$p < 0.05$, ****$p < 0.0001$).

activation by enhancing transcription of key autophagy-related genes like *ATG9A* and *GABARAP* required for the autophagosomes and autolysosomes formation [27,62]. The reduced expression of these genes adds further validity to our hypothesis that patients' cells may have a dysfunctional autophagy pathway. Interestingly, either *NEAT1* silencing or miR-29b overexpression can prevent *NEAT1*'s beneficial effects on autophagy [27,63]. Based on these studies and our expression data, we can reasonably speculate that an abnormal axis involving miR-29 family members and *NEAT1* may influence the autophagy pathway in vEDS cells. Future research targeting miR-29a and miR-29b is likely to provide valuable insights regarding their impact on the defective autophagy that may underpin vEDS.

Dysregulation of miRNAs and lncRNAs may disrupt the ECM architecture and VSMC phenotype, impacting vascular remodeling [64–66]. Accumulated evidence reported that various miRNAs and lncRNAs, including those aberrantly expressed in vEDS like miR-21-3p, miR-24, miR-29a-3p, miR-29b-3p, miR-138, miR-145, miR-195, and *NEAT1*, may play a significant role in altering various ECM structural components of the blood vessels wall, as well as regulating the phenotypic transformation of VSMCs [15,65,67]. miRNAs are important intracellular regulators that target a multitude of genes involved in VSMC apoptosis, elastogenesis, ECM breakdown, and collagen and fibrillins deposition [66,68]. Extensive experimental research has shown that they have potential to disrupt vascular homeostasis and interfere with critical cellular processes linked to vascular diseases, including aneurysmal pathologies [24,68–76]. Given the crucial regulatory role of miR-29 family members in vascular biology [24,67,70], functionally elucidating the marked upregulation of miR-29b in vEDS cells could clarify its contribution in molecular mechanisms underlying the vascular pathogenesis of the disease. Our assumption is supported by well-established scientific evidence linking miR-29b dysregulation, aortic dilation, and aneurysm development. Some research provided in vitro and in vivo experimental data demonstrating miR-29b's contribution to aneurysm formation through its detrimental effects on vascular ECM remodeling [71,72,77,78]. In murine models of abdominal aortic aneurysms, miR-29b upregulation accelerated aneurysm expansion and increased rupture rates. This was accompanied by a decreased expression of known ECM targets (e.g., *Col1a1*, *Col3a1*, *Col5a1*, *Eln*). Conversely, inhibiting miR-29b attenuated aortic aneurysms progression [71]. Similarly, in a mouse model of Marfan syndrome, the expression of miR-29b was found upregulated in the ascending aorta, leading to enhanced matrix metalloproteinase 2 activity and increased elastin fragmentation [72]. Importantly, elevated levels of miR-29b were observed in aortic biopsy samples from patients with thoracic aneurysms [77]. Moreover, miR-29b may act in concert with members of the miR-15 family, such as miR-195, to synergistically control ECM remodeling in blood vessels [79]. Interestingly, long-term suppression of miR-29b was shown to slow the formation and growth of aneurysms

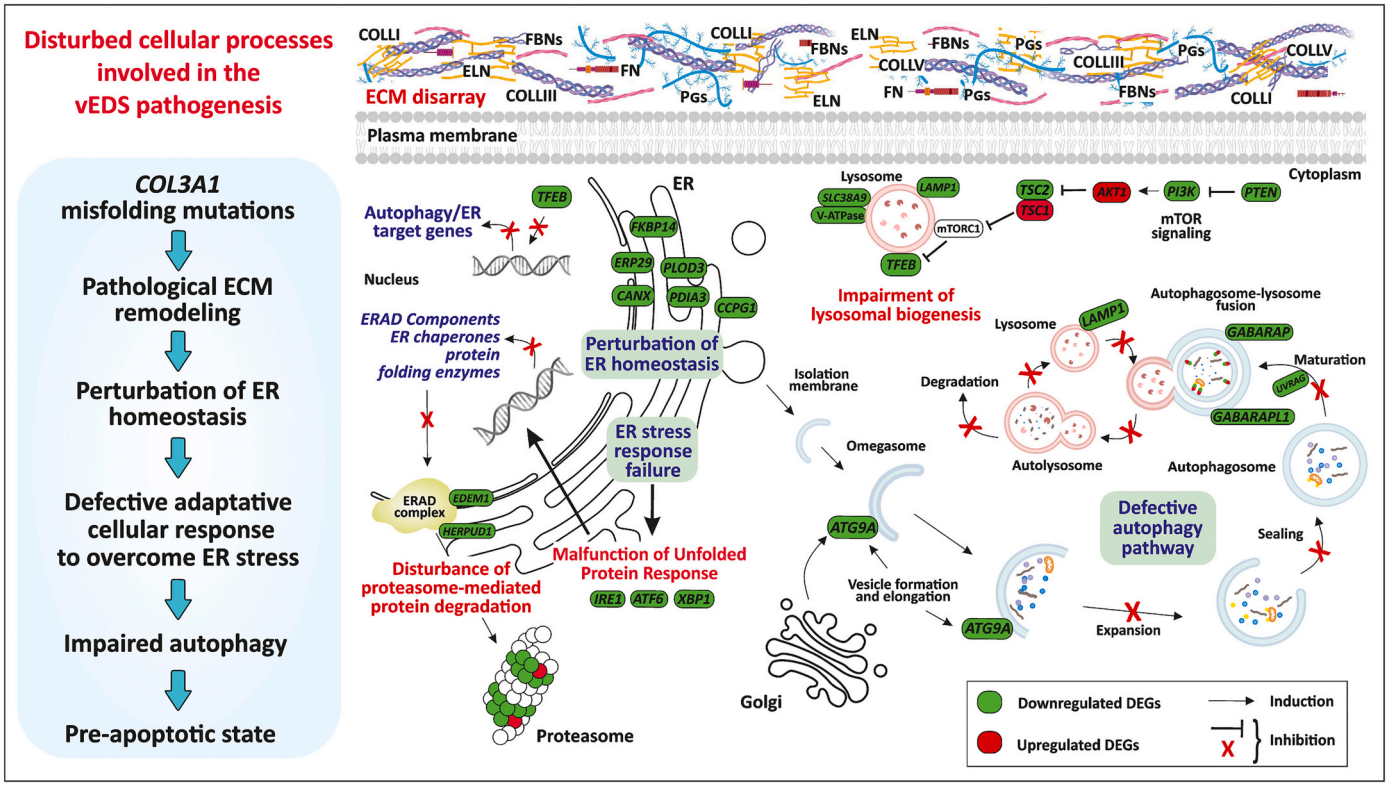

Fig. 7. A schematic overview depicting dysregulated cellular processes in vEDS pathogenesis, based on current and previous research [13,32]. The model highlights key transcriptomic changes that impact these processes. *COL3A1* structural mutations lead to the production of defective COLLIII molecules that cause a widespread ECM disarray. Accumulation of these misfolded aggregates can disturb ER proteostasis, adaptative responses to counteract ER stress (UPR and ERAD pathways), autophagy, the mTOR pathway, and lysosome function through changes in gene expression. Perturbation of these key processes can further impact a range of cell functions like differentiation, proliferation, and apoptosis. Abbreviations: COLLI: type I collagen; COLLIII: type III collagen, COLLV: type V collagen; ECM: extracellular matrix; ELN: elastin; ER: endoplasmic reticulum; ERAD: ER-associated degradation; FBNs: fibrillins; FN: fibronectin; PGs: proteoglycans; UPR: unfolded protein response. The image was created with BioRender.com.

[80], providing compelling evidence for its potential as a therapeutic target in various vasculopathies [24,67,81]. Based on these experimental proofs, it is reasonable to hypothesize that miR-29b may play a key pathogenetic role in vEDS by negatively impacting vascular remodeling, interfering with the ECM structural integrity, and resulting in pathological arterial wall remodeling and vascular fragility. Future research focusing on inhibiting miR-29b activity may aid in understanding how it affects the abnormal remodeling of several essential ECM components like fibrillar collagens, fibrillins, EMILINs, and elastin, which have been shown to be disorganized within the ECM of vEDS fibroblasts [13,32]. Given the crucial roles of miR-21, miR-24, miR-138, and miR-145 in vascular development and homeostasis [24,68,81], these miRNAs are of particular interest for further research into their potential contribution in the vascular signaling mechanisms associated with vEDS. miR-21 overexpression directly targets PTEN and Bcl-2 proteins, regulating VSMC proliferation and apoptosis, and enhancing vessel wall stability [56]. Similarly, elevated levels of miR-24, which exhibited reduced expression in vEDS cells, have been shown to limit aortic vascular inflammation and ECM degradation by affecting macrophage survival and cytokine production [82]. The miR-143/145 cluster and miR-138 both play crucial roles in maintaining VSMC differentiation, promoting their proliferation, migration, and maturation during development [83,84].

5. Conclusions

In summary, the current transcriptome findings significantly enhance our understanding of the pathobiology of vEDS, particularly in light of the limited molecular data available on expression alterations of miRNAs and lncRNAs in this context. Our data help elucidate some key biological aspects, highlighting the involvement of critical cellular and molecular pathways that are intrinsically linked to the underlying pathomolecular mechanisms of vEDS. It is particularly intriguing to note that disruptions in ER proteostasis, impairments in the ER stress response, and dysfunctional autophagy may each play significant roles in disease mechanisms. These findings raise several new research questions that warrant further investigation. For instance, exploring autophagy and ER stress-related pathways as potential targets could yield promising results. Modulating these critical biological functions, for example by increasing autophagic flux, reducing the load of cytotoxic misfolded protein aggregates, and restoring ER functions, may offer therapeutic benefits. A deeper understanding of these interconnected cellular events could provide valuable clues for future translational studies, which may involve restoring collagen proteostasis and ECM functions, both pivotal for maintaining vascular integrity. Our findings also underscore the crucial necessity of elucidating the functional roles that miRNAs and lncRNAs play in vEDS pathogenesis. Of particular interest is our discovery that miR-29b might adversely influence the autophagic pathway and ECM remodeling. Functionally examining miR-29b as a possible molecular target is paramount for unraveling its mechanisms of action and establishing its impact on vascular alterations. All these research efforts could potentially pave the way for new therapeutic approaches in managing vEDS.

Supplementary data to this article can be found online at https://doi.org/10.1016/j.bbadis.2023.166915.

Funding

This work was supported by Fondazione Telethon and the "Associazione con Giacomo contro vEDS", (Grant number: GSA21F001, Seed Grant Fall 2021 vEDS) to Nicola Chiarelli.

CRediT authorship contribution statement

Nicola Chiarelli: Conceptualization, Formal analysis, Investigation, Data curation, Writing – original draft, Writing – review & editing, Visualization, Supervision, Project administration, Funding acquisition. **Valeria Cinquina:** Formal analysis, Investigation, Data curation, Validation, Writing – review & editing, Visualization. **Paolo Martini:** Software, Formal analysis, Investigation, Writing – review & editing. **Valeria Bertini:** Investigation, Validation. **Nicoletta Zoppi:** Investigation, Writing – review & editing. **Marina Venturini:** Resources, Writing – review & editing. **Marco Ritelli:** Conceptualization, Writing – review & editing, Supervision, Project administration. **Marina Colombi:** Conceptualization, Writing – review & editing, Resources, Supervision, Project administration.

Declaration of competing interest

The authors declare no conflict of interest.

Data availability

Data generated or analyzed during this study are included in this published article and its Supplementary Materials. RNA-seq and miRNA-seq data has been deposited into the Gene Expression Omnibus under accession code: GSE239914 and GSE239908.

Acknowledgement

The authors would like to thank Jelena Skripac for her skillful technical assistance. We would like to express our gratitude to the Fazzo Cusan family for their generous support. Part of the funding for Nicola Chiarelli's current appointment as an Assistant Professor at the University of Brescia has been kindly provided by the Fazzo Cusan family.

References

[1] P.H. Byers, J. Belmont, J. Black, J. De Backer, M. Frank, X. Jeunemaitre, D. Johnson, M. Pepin, L. Robert, L. Sanders, N. Wheeldon, Diagnosis, natural history, and management in vascular Ehlers–Danlos syndrome, Am. J. Med. Genet. Part C Semin. Med. Genet. 175 (2017) 40–47.
[2] M.G. Pepin, U. Schwarze, K.M. Rice, M. Liu, D. Leistritz, P.H. Byers, Survival is affected by mutation type and molecular mechanism in vascular Ehlers-Danlos syndrome (EDS type IV), Genet. Med. 16 (2014) 881–888.
[3] M. Ritelli, C. Rovati, M. Venturini, N. Chiarelli, V. Cinquina, M. Castori, M. Colombi, Application of the 2017 criteria for vascular Ehlers-Danlos syndrome in 50 patients ascertained according to the Villefranche nosology, Clin. Genet. 97 (2020) 287–295.
[4] F. Malfait, C. Francomano, P. Byers, J. Belmont, B. Berglund, J. Black, L. Bloom, J. M. Bowen, A.F. Brady, N.P. Burrows, M. Castori, H. Cohen, M. Colombi, S. Demirdas, J. De Backer, A. De Paepe, S. Fournel-Gigleux, M. Frank, N. Ghali, C. Giunta, et al., The 2017 international classification of the Ehlers–Danlos syndromes, Am. J. Med. Genet. Part C Semin. Med. Genet. 175 (2017) 8–26.
[5] L.T. Smith, U. Schwarze, J. Goldstein, P.H. Byers, Mutations in the COL3A1 Gene Result in the Ehlers–Danlos Syndrome Type IV and Alterations in the Size and Distribution of the Major Collagen Fibrils of the Dermis, J. Invest. Dermatol. 108 (1997) 241–247.
[6] M. Frank, J. Albuisson, B. Ranque, L. Golmard, J.M. Mazzella, L. Bal-Theoleyre, A. L. Fauret, T. Mirault, N. Denarié, E. Mousseaux, P. Boutouyrie, J.N. Fiessinger, J. Emmerich, E. Messas, X. Jeunemaitre, The type of variants at the COL3A1 gene associates with the phenotype and severity of vascular Ehlers-Danlos syndrome, Eur. J. Hum. Genet. 23 (2015) 1657–1664.
[7] S. Shalhub, J.H. Black, A.C. Cecchi, Z. Xu, B.F. Griswold, H.J. Safi, D.M. Milewicz, N.B. McDonnell, Molecular diagnosis in vascular Ehlers-Danlos syndrome predicts pattern of arterial involvement and outcomes, J. Vasc. Surg. 60 (2014) 160–169.
[8] R. Omar, F. Malfait, T. Van Agtmael, Four decades in the making: collagen III and mechanisms of vascular Ehlers Danlos syndrome, Matrix Biol. Plus 12 (2021).
[9] R. Vroman, A.-M. Malfait, R.E. Miller, F. Malfait, D. Syx, Animal models of Ehlers–Danlos syndromes: phenotype, pathogenesis, and translational potential, Front. Genet. 12 (2021) 1610.
[10] C.J. Bowen, J.F.C. Giadrosic, Z. Burger, G. Rykiel, E.C. Davis, M.R. Helmers, K. Benke, E.G. MacFarlane, H.C. Dietz, Targetable cellular signaling events mediate vascular pathology in vascular Ehlers-Danlos syndrome, J. Clin. Invest. 130 (2019) 686.
[11] A. Legrand Id, C. Guery, J. Faugeroux, E. Fontaine Id, C. Beugnon, A. Lie Gianfermi, I. Loisel-Ferreiraid, M.-C. Verpont, S. Adhamid, T. Mirault Id, J. Hadchouel, X. Jeunemaitreid, Comparative Therapeutic Strategies for Preventing Aortic Rupture in a Mouse Model of Vascular Ehlers-Danlos Syndrome, 2022.
[12] N. Chiarelli, M. Ritelli, N. Zoppi, M. Colombi, Cellular and molecular mechanisms in the pathogenesis of classical, vascular, and hypermobile ehlers–danlos syndromes, Genes (Basel) 10 (2019).
[13] N. Chiarelli, G. Carini, N. Zoppi, M. Ritelli, M. Colombi, Transcriptome analysis of skin fibroblasts with dominant negative COL3A1 mutations provides molecular insights into the etiopathology of vascular Ehlers-Danlos syndrome, PloS One 13 (2018).
[14] S. Ishikawa, T. Kosho, T. Kaminaga, M. Miyamoto, Y. Hamasaki, S. Yoshihara, S. Hayashi, K. Igawa, Endoplasmic reticulum stress and collagenous formation anomalies in vascular-type Ehlers-Danlos syndrome via electron microscopy, J. Dermatol. 48 (2021) 481–485.
[15] K. Mangum, K. Gallagher, F.M. Davis, The role of epigenetic modifications in abdominal aortic aneurysm pathogenesis, Biomolecules 12 (2022).
[16] A.E. Pasquinelli, MicroRNAs and their targets: recognition, regulation and an emerging reciprocal relationship, Nat. Rev. Genet. 13 (2012) 271–282.
[17] M. Ritelli, N. Chiarelli, V. Cinquina, N. Zoppi, V. Bertini, M. Venturini, M. Colombi, RNA-seq of dermal fibroblasts from patients with hypermobile Ehlers– Danlos syndrome and hypermobility spectrum disorders supports their categorization as a single entity with involvement of extracellular matrix degrading and proinflammatory pathomec, Cells 11 (2022) 4040 (11 (2022) 4040).
[18] R.K.Y. Wong, M. MacMahon, J.V. Woodside, D.A. Simpson, A comparison of RNA extraction and sequencing protocols for detection of small RNAs in plasma, BMC Genomics 20 (2019) 1–12.
[19] M.R. Friedländer, S.D. MacKowiak, N. Li, W. Chen, N. Rajewsky, miRDeep2 accurately identifies known and hundreds of novel microRNA genes in seven animal clades, Nucleic Acids Res. 40 (2012) 37–52.
[20] M.I. Love, W. Huber, S. Anders, Moderated estimation of fold change and dispersion for RNA-seq data with DESeq2, Genome Biol. 15 (2014) 1–21.
[21] B.T. Sherman, M. Hao, J. Qiu, X. Jiao, M.W. Baseler, H.C. Lane, T. Imamichi, W. Chang, DAVID: a web server for functional enrichment analysis and functional annotation of gene lists (2021 update), Nucleic Acids Res. 50 (2022) W216–W221.
[22] G. Bindea, B. Mlecnik, H. Hackl, P. Charoentong, M. Tosolini, A. Kirilovsky, W. H. Fridman, F. Pagès, Z. Trajanoski, J. Galon, ClueGO: a Cytoscape plug-in to decipher functionally grouped gene ontology and pathway annotation networks, Bioinformatics 25 (2009) 1091–1093.
[23] L. Chang, G. Zhou, O. Soufan, J. Xia, miRNet 20: network-based visual analytics for miRNA functional analysis and systems biology, Nucleic Acids Res. 48 (2020) W244–W251.
[24] J. Raffort, F. Lareyre, M. Clement, Z. Mallat, Micro-RNAs in abdominal aortic aneurysms: insights from animal models and relevance to human disease, Cardiovasc. Res. 110 (2016) 165–177.
[25] A.J. Kriegel, Y. Liu, Y. Fang, X. Ding, M. Liang, The miR-29 family: genomics, cell biology, and relevance to renal and cardiovascular injury, Physiol. Genomics 44 (2012) 237–244.
[26] M. Horita, C. Farquharson, L.A. Stephen, The role of miR-29 family in disease, J. Cell. Biochem. 122 (2021) 696.
[27] Y. Kong, T. Huang, H. Zhang, Q. Zhang, J. Ren, X. Guo, H. Fan, L. Liu, The lncRNA NEAT1/miR-29b/Atg9a axis regulates IGFBPrP1-induced autophagy and activation of mouse hepatic stellate cells, Life Sci. 237 (2019).
[28] H.Y. Huang, Y.C.D. Lin, S. Cui, Y. Huang, Y. Tang, J. Xu, J. Bao, Y. Li, J. Wen, H. Zuo, W. Wang, J. Li, J. Ni, Y. Ruan, L. Li, Y. Chen, Y. Xie, Z. Zhu, X. Cai, X. Chen, et al., miRTarBase update 2022: an informative resource for experimentally validated miRNA–target interactions, Nucleic Acids Res. 50 (2022) D222–D230.
[29] J.J. Kwon, J.A. Willy, K.A. Quirin, R.C. Wek, M. Korc, X.M. Yin, J. Kota, Novel role of miR-29a in pancreatic cancer autophagy and its therapeutic potential, Oncotarget 7 (2016) 71635–71650.
[30] J.F. Bateman, M.D. Shoulders, S.R. Lamandé, Collagen misfolding mutations: the contribution of the unfolded protein response to the molecular pathology, Connect. Tissue Res. 63 (2022) 210–227.
[31] J.F. Bateman, R.P. Boot-Handford, S.R. Lamandé, Genetic diseases of connective tissues: cellular and extracellular effects of ECM mutations, Nat. Rev. Genet. 10 (2009) 173–183.
[32] N. Zoppi, R. Gardella, A. De Paepe, S. Barlati, M. Colombi, Human fibroblasts with mutations in COL5A1 and COL3A1 genes do not organize collagens and fibronectin in the extracellular matrix, Down-regulate α2β1 integrin, and recruit αvβ3 instead of α5β1 integrin, J. Biol. Chem. 279 (2004) 18157–18168.
[33] R. Besio, G. Iula, N. Garibaldi, L. Cipolla, S. Sabbioneda, M. Biggiogera, J.C. Marini, A. Rossi, A. Forlino, 4-PBA ameliorates cellular homeostasis in fibroblasts from osteogenesis imperfecta patients by enhancing autophagy and stimulating protein secretion, Biochim. Biophys. Acta Mol. basis Dis. 2018 (1864) 1642–1652.
[34] S.R. Lamandé, Collagen VI muscle disorders: mutation types, pathogenic mechanisms and approaches to, Therapy (2021) 311–323.
[35] S.R. Lamandé, J.F. Bateman, Genetic disorders of the extracellular matrix, Anat. Rec. 303 (2020) 1527–1542.

[36] S. Metti, L. Gambarotto, M. Chrisam, M. Baraldo, P. Braghetta, B. Blaauw, P. Bonaldo, The polyphenol pterostilbene ameliorates the myopathic phenotype of collagen VI deficient mice via autophagy induction, Front. Cell Dev. Biol. 8 (2020).
[37] V. Abbonante, A. Malara, M. Chrisam, S. Metti, P. Soprano, C. Semplicini, L. Bello, V. Bozzi, M. Battiston, A. Pecci, E. Pegoraro, L. De Marco, P. Braghetta, P. Bonaldo, A. Balduini, Lack of COL6/collagen VI causes megakaryocyte dysfunction by impairing autophagy and inducing apoptosis, Autophagy 19 (2023) 984–999.
[38] S. Peña-Llopis, S. Vega-Rubin-De-Celis, J.C. Schwartz, N.C. Wolff, T.A.T. Tran, L. Zou, X.J. Xie, D.R. Corey, J. Brugarolas, Regulation of TFEB and V-ATPases by mTORC1, EMBO J. 30 (2011) 3242–3258.
[39] A. Gebrie, Transcription factor EB as a key molecular factor in human health and its implication in diseases, SAGE Open Med. 11 (2023).
[40] C. Settembre, C. Di Malta, V.A. Polito, M.G. Arencibia, F. Vetrini, S. Erdin, S. U. Erdin, T. Huynh, D. Medina, P. Colella, M. Sardiello, D.C. Rubinsztein, A. Ballabio, TFEB links autophagy to lysosomal biogenesis, Science 332 (2011) 1429.
[41] A. Roczniak-Ferguson, C.S. Petit, F. Froehlich, S. Qian, J. Ky, B. Angarola, T. C. Walther, S.M. Ferguson, The transcription factor TFEB links mTORC1 signaling to transcriptional control of lysosome homeostasis, Sci. Signal. 5 (2012) ra42.
[42] J.A. Martina, Y. Chen, M. Gucek, R. Puertollano, MTORC1 functions as a transcriptional regulator of autophagy by preventing nuclear transport of TFEB, Autophagy 8 (2012) 903–914.
[43] M. Palmieri, S. Impey, H. Kang, A. di Ronza, C. Pelz, M. Sardiello, A. Ballabio, Characterization of the CLEAR network reveals an integrated control of cellular clearance pathways, Hum. Mol. Genet. 20 (2011) 3852–3866.
[44] C. Fung, R. Lock, S. Gao, E. Salas, J. Debnath, Induction of autophagy during extracellular matrix detachment promotes cell survival, Mol. Biol. Cell 19 (2008) 797–806.
[45] A. Avivar-Valderas, E. Bobrovnikova-Marjon, J. Alan Diehl, N. Bardeesy, J. Debnath, J.A. Aguirre-Ghiso, Regulation of autophagy during ECM detachment is linked to a selective inhibition of mTORC1 by PERK, Oncogene 32 (2013) (2012) 4932–4940.
[46] Y. Ishida, A. Yamamoto, A. Kitamura, S.R. Lamandé, T. Yoshimori, J.F. Bateman, H. Kubota, K. Nagata, Autophagic elimination of misfolded procollagen aggregates in the endoplasmic reticulum as a means of cell protection, Mol. Biol. Cell 20 (2009) 2744–2754.
[47] F. Iavarone, G. Di Lorenzo, C. Settembre, Regulatory events controlling ER-phagy, Curr. Opin. Cell Biol. 76 (2022).
[48] C. Hetz, E. Chevet, H.P. Harding, Targeting the unfolded protein response in disease, Nat. Rev. Drug Discov. 12 (2013) 703–719.
[49] N. Zoppi, S. Barlati, M. Colombi, FAK-independent αvβ3 integrin-EGFR complexes rescue from anoikis matrix-defective fibroblasts, Biochim. Biophys. Acta-Mol, Cell Res. 1783 (2008) 1177–1188.
[50] N. Zoppi, N. Chiarelli, M. Ritelli, M. Colombi, Multifaced roles of the αvβ3 integrin in Ehlers-Danlos and arterial tortuosity syndromes' dermal fibroblasts, Int. J. Mol. Sci. 19 (2018).
[51] R.A. Saxton, D.M. Sabatini, mTOR signaling in growth, metabolism, and disease, Cell 168 (2017) 960.
[52] S. Sciarretta, M. Forte, G. Frati, J. Sadoshima, New insights into the role of mtor signaling in the cardiovascular system, Circ. Res. 122 (2018) 489–505.
[53] R. Bartolomeo, L. Cinque, C. De Leonibus, A. Forrester, A.C. Salzano, J. Monfregola, E. De Gennaro, E. Nusco, I. Azario, C. Lanzara, M. Serafini, B. Levine, A. Ballabio, C. Settembre, mTORC1 hyperactivation arrests bone growth in lysosomal storage disorders by suppressing autophagy, J. Clin. Invest. 127 (2017) 3717–3729.
[54] T. Sun, M.Y. Li, P.F. Li, J.M. Cao, MicroRNAs in cardiac autophagy: small molecules and big role, Cells 7 (2018) 1–15.
[55] D. Corà, F. Bussolino, G. Doronzo, TFEB signalling-related microRNAs and autophagy, Biomol. 11 (2021) 985 (11 (2021) 985).
[56] L. Maegdefessel, J. Azuma, R. Toh, A. Deng, D.R. Merk, A. Raiesdana, N.J. Leeper, U. Raaz, A.M. Schoelmerich, M.V. McConnell, R.L. Dalman, J.M. Spin, P.S. Tsao, MicroRNA-21 blocks abdominal aortic aneurysm development and nicotine-augmented expansion, Sci. Transl. Med. 4 (2012).
[57] Y. Zhou, M. Wang, J. Zhang, P. Xu, H. Wang, MicroRNA-29a-3p regulates abdominal aortic aneurysm development and progression via direct interaction with PTEN, J. Cell. Physiol. 235 (2020) 9414–9423.
[58] J. Yu Shi, C. Chen, X. Xu, Q. Lu, miR-29a promotes pathological cardiac hypertrophy by targeting the PTEN/AKT/mTOR signalling pathway and suppressing autophagy, Acta Physiol. 227 (2019).
[59] Y.M. Oh, S.W. Lee, W.K. Kim, S. Chen, V.A. Church, K. Cates, T. Li, B. Zhang, R. E. Dolle, S. Dahiya, S.C. Pak, G.A. Silverman, D.H. Perlmutter, A.S. Yoo, Age-related Huntington's disease progression modeled in directly reprogrammed patient-derived striatal neurons highlights impaired autophagy, Nat. Neurosci. 2022 2511 (25) (2022) 1420–1433.
[60] H. Yamamoto, S. Kakuta, T.M. Watanabe, A. Kitamura, T. Sekito, C. Kondo-Kakuta, R. Ichikawa, M. Kinjo, Y. Ohsumi, Atg9 vesicles are an important membrane source during early steps of autophagosome formation, J. Cell Biol. 198 (2012) 219–233.
[61] Q. Wu, J. Chen, Z. Tan, D. Wang, J. Zhou, D. Li, Y. Cen, Long non-coding RNA (lncRNA) nuclear enriched abundant transcript 1 (NEAT1) regulates fibroblast growth factor receptor substrate 2 (FRS2) by targeting microRNA (miR)-29-3p in hypertrophic scar fibroblasts, Bioengineered 12 (2021) 5210–5219.
[62] H. Tsuchiya, R. Shinonaga, H. Sakaguchi, Y. Kitagawa, K. Yoshida, G. Shiota, NEAT1 confers radioresistance to hepatocellular carcinoma cells by inducing PINK1/Parkin-mediated mitophagy, Int. J. Mol. Sci. 23 (2022).
[63] H. Sakaguchi, H. Tsuchiya, Y. Kitagawa, T. Tanino, K. Yoshida, N. Uchida, G. Shiota, NEAT1 confers radioresistance to hepatocellular carcinoma cells by inducing autophagy through GABARAP, Int. J. Mol. Sci. 23 (2022).
[64] M. Ponticos, B.D. Smith, Extracellular matrix synthesis in vascular disease: hypertension, and atherosclerosis, J. Biomed. Res. 28 (2014) 25–39.
[65] R. Gurung, A.M. Choong, C.C. Woo, R. Foo, V. Sorokin, Genetic and epigenetic mechanisms underlying vascular smooth muscle cell phenotypic modulation in abdominal aortic aneurysm, Int. J. Mol. Sci. 21 (2020) 1–33.
[66] K.B. Rombouts, T.A.R. van Merrienboer, J.C.F. Ket, N. Bogunovic, J. van der Velden, K.K. Yeung, The role of vascular smooth muscle cells in the development of aortic aneurysms and dissections, Eur. J. Clin. Invest. 52 (2022) 13697.
[67] S. Kumar, R.A. Boon, L. Maegdefessel, S. Dimmeler, H. Jo, Role of noncoding RNAs in the pathogenesis of abdominal aortic aneurysm: possible therapeutic targets? Circ. Res. 124 (2019) 619–630.
[68] G. Wang, Y. Luo, X. Gao, Y. Liang, F. Yang, J. Wu, D. Fang, M. Luo, MicroRNA regulation of phenotypic transformations in vascular smooth muscle: relevance to vascular remodeling, Cell. Mol. Life Sci. 80 (2023) 144.
[69] K.-C. Chen, Y.-S. Wang, C.-Y. Hu, W.-C. Chang, Y.-C. Liao, C.-Y. Dai, S.-H.H. Juo, OxLDL up-regulates microRNA-29b, leading to epigenetic modifications of MMP-2/MMP-9 genes: a novel mechanism for cardiovascular diseases, FASEB J. 25 (2011) 1718–1728.
[70] D.M. Milewicz, MicroRNAs, fibrotic remodeling, and aortic aneurysms, J. Clin. Invest. 122 (2012) 490–493.
[71] L. Maegdefessel, J. Azuma, R. Toh, D.R. Merk, A. Deng, J.T. Chin, U. Raaz, A. M. Schoelmerich, A. Raiesdana, N.J. Leeper, M.V. McConnell, R.L. Dalman, J. M. Spin, P.S. Tsao, Inhibition of microRNA-29b reduces murine abdominal aortic aneurysm development, J. Clin. Invest. 122 (2012) 497–506.
[72] D.R. Merk, J.T. Chin, B.A. Dake, L. Maegdefessel, M.O. Miller, N. Kimura, P.S. Tsao, C. Iosef, G.J. Berry, F.W. Mohr, J.M. Spin, C.M. Alvira, R.C. Robbins, M. P. Fischbein, MiR-29b participates in early aneurysm development in Marfan syndrome, Circ. Res. 110 (2012) 312–324.
[73] Y. Li, L. Maegdefessel, Non-coding RNA contribution to thoracic and abdominal aortic aneurysm disease development and progression, Front. Physiol. 8 (2017) 429.
[74] A.S.I. Ahmed, K. Dong, J. Liu, T. Wen, L. Yu, F. Xu, X. Kang, I. Osman, G. Hu, K. M. Bunting, D. Crethers, H. Gao, W. Zhang, Y. Liu, K. Wen, G. Agarwal, T. Hirose, S. Nakagawa, A. Vazdarjanova, J. Zhou, Long noncoding RNA NEAT1 (nuclear paraspeckle assembly transcript 1) is critical for phenotypic switching of vascular smooth muscle cells, Proc. Natl. Acad. Sci. U. S. A. 115 (2018) E8660–E8667.
[75] Z. Yuan Wu, M. Trenner, R.A. Boon, J.M. Spin, L. Maegdefessel, Long noncoding RNAs in key cellular processes involved in aortic aneurysms, Atherosclerosis 292 (2020) 112–118.
[76] K.D. Mangum, M.A. Farber, Genetic and epigenetic regulation of abdominal aortic aneurysms, Clin. Genet. 97 (2020) 815–826.
[77] R.A. Boon, T. Seeger, S. Heydt, A. Fischer, E. Hergenreider, A.J.G. Horrevoets, M. Vinciguerra, N. Rosenthal, S. Sciacca, M. Pilato, P. Van Heijningen, J. Essers, R. P. Brandes, A.M. Zeiher, S. Dimmeler, MicroRNA-29 in aortic dilation: implications for aneurysm formation, Circ. Res. 109 (2011) 1115–1119.
[78] L. Maegdefessel, J. Azuma, P.S. Tsao, MicroRNA-29b regulation of abdominal aortic aneurysm development, Trends Cardiovasc. Med. 24 (2014) 1–6.
[79] A. Zampetaki, R. Attia, U. Mayr, R.S.M. Gomes, A. Phinikaridou, X. Yin, S. R. Langley, P. Willeit, R. Lu, B. Fanshawe, M. Fava, J. Barallobre-Barreiro, C. Molenaar, P.W. So, A. Abbas, M. Jahangiri, M. Waltham, R. Botnar, A. Smith, M. Mayr, Role of miR-195 in aortic aneurysmal disease, Circ. Res. 115 (2014) 857–866.
[80] H. Okamura, F. Emrich, J. Trojan, P. Chiu, A.R. Dalal, M. Arakawa, T. Sato, K. Penov, T. Koyano, A. Pedroza, A.J. Connolly, M. Rabinovitch, C. Alvira, M. P. Fischbein, Long-term miR-29b suppression reduces aneurysm formation in a Marfan mouse model, Physiol. Rep. 5 (2017), e13257.
[81] I.N. Schellinger, A.R. Dannert, K. Mattern, U. Raaz, P.S. Tsao, Unresolved issues in RNA therapeutics in vascular diseases with a focus on aneurysm disease, Front. Cardiovasc. Med. 8 (2021) 1–16.
[82] L. Maegdefessel, J.M. Spin, U. Raaz, S.M. Eken, R. Toh, J. Azuma, M. Adam, F. Nagakami, H.M. Heymann, E. Chernugobova, H. Jin, J. Roy, R. Hultgren, K. Caidahl, S. Schrepfer, A. Hamsten, P. Eriksson, M.V. McConnell, R.L. Dalman, P. S. Tsao, MiR-24 limits aortic vascular inflammation and murine abdominal aneurysm development, Nat. Commun. 5 (2014) 1–13.
[83] L. Elia, M. Quintavalle, J. Zhang, R. Contu, L. Cossu, M.V.G. Latronico, K. L. Peterson, C. Indolfi, D. Catalucci, J. Chen, S.A. Courtneidge, G. Condorelli, The knockout of miR-143 and -145 alters smooth muscle cell maintenance and vascular homeostasis in mice: correlates with human disease, Cell Death Differ. 16 (2009) 1590–1598.
[84] J. Xu, L. Li, H.F. Yun, Y.S. Han, MiR-138 promotes smooth muscle cells proliferation and migration in db/db mice through down-regulation of SIRT1, Biochem. Biophys. Res. Commun. 463 (2015) 1159–1164.